Renewable Energy 189 (2022) 1046–1062

Contents lists available at ScienceDirect

Renewable Energy

journal homepage: www.elsevier.com/locate/renene

A methodology to estimate the photovoltaic potential on parking spaces and water deposits. The case of the Canary Islands

Schallenberg-Rodriguez Julieta [a, *], Rodrigo-Bello José-Julio [b], Yanez-Rosales Pablo [a]

[a] Industrial and Civil Engineering Faculty, Universidad de Las Palmas de Gran Canaria, Spain
[b] Cartográfica de Canarias, S.A., Spain

ARTICLE INFO

Article history:
Received 13 July 2021
Received in revised form
11 January 2022
Accepted 23 February 2022
Available online 2 March 2022

Keywords:
Photovoltaic potential
Water deposits
Parking spaces
Canary islands
Cartographic information

ABSTRACT

In regions where the land available is scarce it is of special interest to deploy solar photovoltaic energy without occupying additional land. Besides solar roofs, which have already been extensively studied, there are other type of constructions that could be used for the deployment of solar photovoltaic such as car parking spaces and big water deposits. No much attention has been given so far to these type of elements that could potentially been used to deploy solar photovoltaic energy. So the aim of this research is to establish how relevant can these type of surfaces be in terms of solar energy production. For this purpose a methodology has been developed to identify the surfaces corresponding to uncovered parking spaces and water deposit at regional level using cartographic information, first, and, secondly, to estimate how much of these areas could be used to deploy solar photovoltaic energy. This methodology has been applied to one insular region, the Canary Islands, and the results are surprising in terms of the potentiality of these type of elements for the deployment of solar photovoltaic energy which could cover around 9% of the whole regional electricity demand.

1. Introduction

The European Union has set the objective of decarbonizing the economy by 2050. This objective has been assumed by Spain, which will try to become a carbon-neutral country by 2050. The Government of the Canary Islands has decided to advance this process to 2040. In this line, a 100% renewable scenario is proposed for the Canary Islands by 2040.

This means moving towards a model entirely based on renewable energy for all energy uses. In order to meet these objectives, the Canary Islands have to exploit its great potential in renewable energies, especially solar and wind energies, which currently account only for 4% of its total primary energy demand and for 16% of its electricity consumption [1]. Thus, currently, the Canary Islands are highly dependent on fossil fuels and, therefore, from abroad.

One of the constraints of the Canary Islands is its limited territory, so the development of solar energy has to be implemented, as far as possible, without using additional land. Hence the need to evaluate the photovoltaic (PV) potential in already built surfaces. In this regard, one of the aims of this paper is to analyse the potential contribution of PV open parking spaces and PV water deposits to the overall goal of achieving 100% RES by 2040 in the Canary Islands and how these surfaces can contribute to reach this Governmental objective.

This territorial limitation is common to many European territories and also, on a global scale, in regions with a high population density, being especially pressing on islands and small island states. Therefore, this article proposes a methodology to evaluate the potential of photovoltaic solar energy on already built surfaces. Photovoltaic roofs are explicitly excluded from this study since there are already numerous scientific publications dedicated to evaluating the photovoltaic potential of roofs in suburbs [1], cities [2–11], islands [12–14], regions [15,16], countries [17–20] or even for entire continents [21].

However, scientific articles that address the PV potential in built areas, except for PV roofs, are scarce. These already built areas are, for example, large parking areas and large water deposits. Only a few articles include studies on parking areas and none of them carry out a joined evaluation of the photovoltaic potential in a given territory. Some articles estimated the photovoltaic potential on uncovered car parking spaces, but only for parking lots whose parking area was already known, so no methodology was developed to estimate the parking area [22,23]. To our best knowledge,

* Corresponding author.
E-mail address: julieta.schallenberg@ulpgc.es (S.-R. Julieta).

https://doi.org/10.1016/j.renene.2022.02.103
0960-1481/

no research has studied so far the PV potential on water deposits.

This research focuses on evaluating the PV potential on open parking spaces and water deposits at a regional scale. To our knowledge this is the first time that such a research has been developed. No article dealing with the PV potential on water deposits has been found in the literature review, neither any article that systematically estimates the open air parking areas for PV purposes in wide geographical areas, such as cities, regions or countries.

2. Methodology

The main objective of this research is to evaluate the available surface on uncovered parking lots and on large water deposits for the exploitation of photovoltaic solar energy, at the regional, island and municipality level.

The methodology used in this research step by step is described below.

Step 1 Calculation method to estimate the solar radiation.
Part 2 Methodology to estimate the available area for the installation of photovoltaic solar energy for each one of the identified surface typologies, namely uncovered parking lots and large water deposits.
Step 3 Methodology for the characterization of the surfaces identified in terms of shadows. Calculation of the Shadow Factor (FS).
Step 4 Methodology for the characterization of the identified surfaces in terms of the useable area for photovoltaic solar installations. Calculation of the Utilization Factor (FU).
Step 5 Methodology to calculate the photovoltaic power that could be installed on the available surfaces.
Step 6 Methodology to calculate the annual, monthly and hourly energy photovoltaic production
Step 7 Impact of the photovoltaic production at island level, potential contribution to 100% RES energy plan, economic impact and additional benefits of the proposed solution.

2.1. Estimation of the solar radiation

2.1.1. Methodologies overview

Accurate knowledge of the solar irradiation is essential for a multitude of applications, including solar power generation systems. Global solar radiation can be measured on the ground using meteorological stations with pyranometers, which are expensive to install and maintain. The development of a solar irradiation map by interpolation/extrapolation only of data from meteorological stations is not appropriate due to the large errors that arise when these stations are nor close neither uniformly distributed.

Solar radiation can also be measured through the analysis of satellite images. Both the resolution of these images, in general of a few km x km, and their variability in terms of cloud cover and microclimatic variables, induce in these models a certain degree of uncertainty that is not known in most cases.

2.1.2. Methodology implemented

The methodology implemented can be summarized as follows.

Step 1 Selection of the satellite databases to be used among the existing ones
Step 2 Solar data collection from meteorological stations, data processing and calculation of annual averages
Step 3 Calibration of database data with pyranometer measurements.

This methodology is described below.

2.1.3. Solar irradiation data

2.1.3.1. Satellite databases. In recent years, a series of databases with information on solar energy resources have been developed. Some of them are ESRA [24,25], SODA [26,27], Satel-Light [28], PVGIS [29–31], PVSAT [32], PVSAT-2 [33,34] or Heliostat [35,36]. This has led to the situation that several different databases exist in parallel, each of them with a different focus, with different spatial and temporal coverages as well as resolutions.

2.1.4. Solar irradiance and irradiation model. Software tool GRASS-rsun

This model computes the direct (beam), diffuse and reflected solar irradiation raster maps for given day, latitude, surface and atmospheric conditions. Solar parameters (e.g. sunrise, sunset times, declination, extra-terrestrial irradiance, daylight length) are saved in the map history file. Alternatively, a local time can be specified to compute solar incidence angle and/or irradiance raster maps. The model is implemented in a GIS software called GRASS.

The r.sun model algorithm is conceptually based on the equations published in ESRA. The direct, diffuse and reflected solar irradiation components are estimated for both the horizontal and the inclined planes. The total daily irradiance [Wh/m2] is calculated by integrating the irradiance values [W/m2] calculated at regular intervals during the day. In each calculation, the shadows due to the terrain are taken into account, which are calculated from digital elevation models. Thus, this model provides daily data, but not annual averaged data [37].

2.1.5. Solar radiation map of the Canary Islands

The problem of all satellite databases is their resolution which, in the best of the cases, is 1 × 1 km2. Thus, it has been decided to use the data from the solar radiation map developed by the company Dobon's Technology for the Canary Islands, whose resolution is 50 × 50 m [38].

This map used the horizontal global radiation data from 97 meteorological stations located in the Canary Islands (data collection periods from 1 to 10 years). These values were fed into a database to obtain the monthly insolation averages. Using the GRASS software and the spline interpolation technique, maps were generated with a resolution of 50 × 50 m. To this end, the digital terrain elevation maps provided by GRAFCAN with a grid resolution of 50 × 50 m were also used. A more detailed description of the model can be found in Ref. [38].

2.1.6. Measured solar radiation data in the Canary Islands

In the Canary Islands, various solar radiation measurement campaigns have been carried out over time for different purposes. Thus, the data sources and their availability is not consistent: data in different periods and intervals, availability sometimes of the mean values only, in some cases the reliability and length of records is unknown.

The institutions that have provided data series are the State Meteorological Agency (AEMET), the Ministry of Agriculture and Fisheries, Food and Environment and private companies/promoters. Data series commonly show some measurement errors. The most common error is that of unmeasured data, meaning that some intervals were not measured. To solve this problem, a code was developed that first creates the gaps of the unmeasured data, and then estimates those data. Two programs were developed in MATLAB code (MATLAB program version R2018b, license 40760023 ULPGC): one to complete data of incomplete series, using cubic interpolations, and another to obtain the corresponding values, using linear or cubic interpolations depending on the data cadence.

Once the series were complete, the annual averages were calculated. These annual averages were ultimately used to compare them with the available solar maps.

2.1.7. Calibration of the solar map using pyranometer measurements

In order to calibrate the radiation maps, two different models were compared, the GRASS-r.sun and the radiation map of the Canary Islands, with the pyranometer data. To check possible correlations between the GRASS-r.sun model and the pyranometer data, and since the GRASS-r.sun provides only daily solar radiation data, 4 days of the year were selected, representative of each season, to make an initial comparison with the selected pyranometer stations.

2.2. Estimation of the available area

The areas that have been selected for this research are the following ones:

- Outdoor parking areas for vehicles that can be covered with photovoltaic solar panels.
- Large water deposits (covered or uncovered)

The selection of these areas has been carried out using the *Element Capture Methods* in both cases, based on photointerpretation techniques and extraction of cartographic elements, but following different procedures, as described below.

The methodology used to identify open parking spaces was different for public and private parking spaces. In the case of public parking spaces, the reference used have been the points of interest layer of "parkings" of the digital street map of the Canary Islands which have been photo-interpreted. For private open-parking spaces the methodology used was based on photointerpretation of the last available orthophoto of urban areas to identify private parking spaces, since these elements do not exist as polygons in the cartography. The digitization has been carried out trying to cover the entire parking area, but excluding the elements that invade it. Additionally, the general criterion was a minimum parking space of 200 square meters. Fig. 1 shows an example of one parking space.

The methodology used to identify water deposits was based on two steps:

Step 1 Use of the layer "deposits" from the regional topographic map.
Step 2 Photointerpretation of the orthophotos to identify and exclude the deposits that are not water deposits, e.g. fuel deposits.

Fig. 2 shows an example of a water deposit.

2.3. Shadow factor (FS) calculation

This section describes the methodology for the characterization of the identified surfaces in terms of shadows, which will ultimately lead to the calculation of the Shadow Factor (FS) for each type of surface.

Due to the urban nature of most of the selected items, especially the parking spaces but also some deposits, the calculation of the radiation losses due to the shadows projected by the nearby objects (buildings, trees …) is critical.

Fig. 3 shows an example of the enormous effect of the projected shadows on a parking space shown in the orthophoto.

To quantify the radiation loss due to shadows on each enclosure a very detailed model of the objects located above the ground level is required as well as the calculation of the solar radiation during several days of the year along the whole day. This will ultimately lead to the calculation of the Shadow Factor (SF).

Fig. 1. Examples of the element "parking spaces".

The information from the LIDAR (Light Detection and Ranging) sensor available for the Canary Islands was used to model the objects on the ground. This LIDAR provides a detailed net of points, whose nominal resolution is 1 point/square meter, that contains both the ground elements and the objects above the ground.

The LIDAR is an airborne laser sensor able to provide a georeferenced cloud of points of the territory. The sensor measures the time that the laser needs to be emitted, hit the ground and return to the sensor. Since the exact position and orientation of the plane is known, the coordinates (x, y, z) of each of the points can be calculated. Fig. 4 shows an example of the operation of this LIDAR.

The r.sun tool, from the GRASS GIS software package, has been used to calculate the solar irradiation. The r.sun is a solar irradiance and irradiation model that computes direct (beam), diffuse and reflected solar irradiation raster maps for a given day, latitude, surface and atmospheric conditions. Additionally, a local time can

Fig. 2. Examples of the element "water deposit".

Fig. 3. Example of the shadow effect on a parking space (orthophoto).

be specified to compute solar incidence angle and/or irradiance raster maps. The shadowing effect of the topography is incorporated by default. This can be done either internally by calculation of the shadowing effect directly from the digital elevation model or by specifying raster maps of the horizon height which is much faster [37].

Fig. 5 shows an example of a detailed calculation of the solar irradiation with the r.sun tool and the Lidar surface model.

This method allows the calculation of the accumulated solar irradiation during a day (integration every 30 min) using a digital terrain model. Default parameters of albedo (0.2) and atmospheric turbidity (Linke atmospheric turbidity) 3.0 have been used, which are the verified values for the Canary Islands [39].

The r.sun tool allows the calculation of absolute irradiation values, but, in this case, it has been used to calculate the irradiation loss due to the shadows (a correction factor that will be later applied to the solar radiation model chosen for the Canary Islands). For this purpose, the solar irradiation has been calculated twice. The first time this calculation is done taking into account the objects on the ground (buildings, trees, etc.) and the second time without taking them into account. To do this, own produced classified LIDAR files are used. These LIDAR files result in a cloud of points. Within the classification used in these files there is one type called "soil", by activating the class “2”, one can filter the cloud of points that are ground (soil) and by deactivating it, one will get all the cloud of points, meaning the ground plus trees, buildings, etc. By using this procedure, it was possible to calculate the solar irradiation difference between both maps and, thus, the shadow factor (FS).

Due to the complexity and time requirements of the calculations, it has been decided to select four days of the year as representative of each of the 4 seasons and to use their average to calculate the annual solar irradiation losses. For this purpose, the following days have been selected: day 80, day 172, day 264 and day 355.

The first step consisted in the generation of the digital terrain models from the information of the LIDAR points. Two models were generated, one digital surface model that includes all the elements above the terrain (buildings, trees …) and a second digital terrain model without the objects on top of the ground. Both models were calculated at a resolution of 5m/pixel for all areas included in this study (uncovered parking spaces and large deposits).

The r.sun tool was run for each of the enclosures twice, once for each of the two models, and the irradiation was calculated for the 4 selected days of the year in each case. Thus, the annual mean radiation loss factor due to shadows was calculated.

To our knowledge, this procedure to calculate the Shadow Factor as it is described above, is the first time that has been described in an article.

2.4. Utilization factor (UF) calculation

This section describes the methodology used to characterize the identified surfaces in terms of their useable area for photovoltaic solar installations, which will ultimately lead to the calculation of the Utilization Factor (FU) for each type of surface.

2.4.1. Part 1. Utilization factor (UF)

2.4.1.1. Utilization factor in parking areas. To estimate a realistic average utilization factor in parking areas, different real examples of uncovered parking spaces where a photovoltaic installation was already in place were studied. Fig. 6 shows an example for comparison purposes, which is the INFECAR car parking space in Las Palmas de Gran Canaria, where the right half is already covered

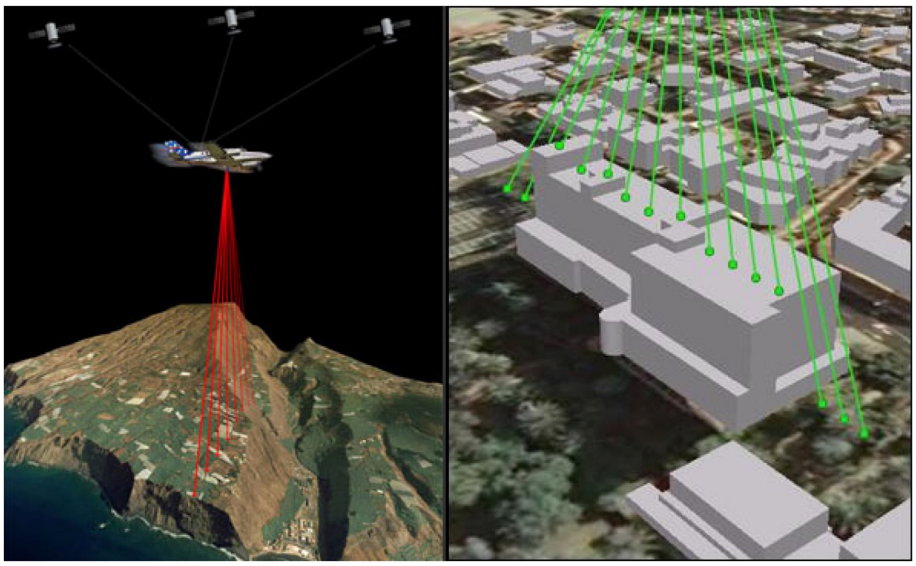

Fig. 4. Example of the operation of the LIDAR.

Fig. 5. Example of calculation of solar irradiation with r.sun and LIDAR.

with photovoltaic panels and the left side is still to be covered.

After a comprehensive analysis of several photovoltaic parking projects, the selected utilization factor was 35%, a value that is considered realistic but also conservative.

2.4.1.2. Utilization factor in deposits. To estimate a realistic average utilization factor in water deposits (covered or uncovered), different examples of deposits where a photovoltaic installation was already in place were studied. Fig. 7 shows an example of an uncovered deposit with a photovoltaic installation in Arinaga (Gran Canaria).

After a comprehensive analysis of several photovoltaic water deposit projects, the selected utilization factor was 40%, a value that is considered realistic but on the conservative side.

2.5. Methodology to calculate the photovoltaic power

This section describes the methodology used to calculate the photovoltaic power that can be installed on the identified surfaces.

To find the installable power, the Surface/Power ratio is multiplied by the useable area. The useable area is the result of multiplying the available area by the corresponding utilization factor.

The equation to determine the photovoltaic power follows:

$$P\,(kW) = UF \cdot S\,(m2) \,/\, (S/P) \quad (1)$$

Where:

P (kW): Power (kW)
S: Available Surface (m2)

Fig. 6. Photovoltaic parking space in INFECAR (Gran Canaria).

S/P: Surface/Power ratio (m2/kW)

This Surface/Power ratio is estimated as follows.

2.5.1. Estimation of the surface/power ratio (S/P)

To estimate the efficiency and the Surface/Power ratio of the photovoltaic panel, several catalogues of the latest generation polycrystalline and monocrystalline silicon photovoltaic panels were consulted. Their main parameters are shown in Table 1.

The PV panels that had an efficiency below 20% were not considered in this study (dark shaded rows in Table 1). For the remaining panels, the calculated Surface/Power ratio was between 4.42 and 4.94. As shown in Table 1, the higher the performance, the lower the Surface/Power ratio. In this study, the Surface/Power ratio has been prioritized, which is why the SunForte PM096B00 Panel was finally selected whose main parameters are: power 330 W, efficiency 20.3% and Surface/Power ratio 4.94 m2/kW.

2.6. Method to calculate the PV production

This section describes the methodology used to calculate the annual photovoltaic production that could be installed on the identified areas. The photovoltaic solar production has been calculated as per equation (2).

$$P = \frac{365 \cdot IG_{tilt} \cdot \varepsilon \cdot PR \cdot S \cdot SF \cdot UF}{10^6} \quad (2)$$

Where:

P : *Production*(MWh/a)
IG_{tilt} : Solar *radiation on tilted surfaces*$(Wh/(m^2 \cdot \mathrm{d})$
ε : *Panel efficiency*
PR : *PerformanceRatio*
S : *Total area of panels*(m^2)
SF: Shadow Factor
UF: Utilization Factor

The increase of the solar radiation on tilted areas (average tilt around 20%) with respect to the horizontal solar radiation was estimated in ca. 8%. The Performance Ratio (PR) considered was 0.8. The shadow factors were calculated for each of the identified enclosures, as specified in the previous sections. The utilization factors for each identified typology, namely parking spaces an water deposits, as specified in the previous sections. The efficiency of the selected panel, SunForte PM096B00, is 20.3% (see Table 1).

The yearly PV production has been calculated using GIS by crossing the solar radiation map and the map of the resulting surfaces.

The hourly PV production has been estimated using the series of pyranometer data for each island. The monthly PV productions have been calculated aggregating the hourly PV production data.

2.7. Impact of the photovoltaic production at island level and additional benefits of the proposed solution

This section describes the impact of the proposed solution at two different levels:

1. The impact of the photovoltaic production at island level and potential contribution to the island' energy plan

Fig. 7. Uncovered water deposit with a photovoltaic installation in Arinaga (Gran Canaria).

Table 1
Main parameters of photovoltaic panels.

Manufacturer	Model	Efficiency	Power	Size (mm^2)	S/P (m^2/kW)
SunPower	SPR-X22-370 (Ahora MAX3-400)	22.6%	400W	1690 × 1046	4.42
SunPower	SPR-X22-360 (Ahora MAX3-390)	22.1%	390W	1690 × 1046	4.53
SunPower	MAX3-370	20.9%	370W	1690 × 1046	4.78
LG Neon	LG360Q1C-A5	20.8%	360W	1700 × 1016	4.80
LG	LG355Q1C-A5	20.6%	355W	1700 × 1016	4.87
AUO	SunForte PM096B00	20.6%	335W	1559 × 1046	4.87
SunPower	MAX2-360	20.4%	360W	1690 × 1046	4.91
AUO	SunForte PM096B00	20.3%	330W	1559 × 1046	4.94
SunPower	MAX3-350	19.8%	327W	1690 × 1046	
SHARP	NQ-R256A	19.8%	256W	1318 × 980	
Panasonic	VBHN330SJ53	19.7%	330W	1590 × 1053	
Panasonic	VBHN325SJ53	19.4%	325W	1590 × 1053	
SunPower	SPR-P19-400	19.4%	400W	2067 × 998	

2. Other impacts: economic impact and additional benefits

2.7.1. Impact of the photovoltaic production at island level

In this subsection several indicators will be analysed as the percentage of the annual insular demand that could be supplied by photovoltaic energy and the resulting PV surface to be installed on parking spaces an water deposits. These indicators will be contextualised for each island, indicating relevant islands' parameters such as total surface, total population, per capita electricity consumption and electricity growth rate, in order to estimate the real impact of the proposed solutions at the island level, as well as its potential contribution to the island' energy plan.

2.7.2. Economic impact

One common benefit for open parking spaces and on water deposits is the economic benefit associated to the price at which the solar electricity produced could be sold in the electricity market. Open parking spaces and water deposits are surfaces already used for one purpose, to park cars in the first case and to store water in the second one, and the photovoltaic structures will add an additional purpose to these areas: the production of electricity without occupying additional space. This electricity produces will be fed into the electrical grid generating an additional economic benefit for the promoters.

The methodology used to evaluate the economic impact of the photovoltaic installations is based on the estimation of the Net Present Value (NPV), total benefit and annualized benefit, Internal Rate of Return (IRR) and the payback.

The NPV estimated the total profit or loss of a project throughout its lifetime (in absolute terms) updated to the year 0, that is, the year in which the project is commissioned. The NPV has been calculated using equations (3)–(6).

$$NPV = -C_i + \sum_{t=1}^{n} \frac{F_t}{(1+k)^t} \tag{3}$$

$$C_i : P_i \times p_u \tag{4}$$

$$F_t = I_t - C_t \tag{5}$$

$$I_t : P_r \times p_{ue} \tag{6}$$

Where:

NPV = Net Present Value
C_i: Capital investment cost of each island (€M)
P_i: Power installed on each island (MW)
p_u: Unit price of investment (€M/MW)
n: lifetime (years)
t: Every year in which the calculation of the flow and updating of the money is carried out
F_t: Annual cash flow (€M)
I_t: Annual income (€M)
P_r: Average annual production of each wind farm (MWh)
p_{ue}: Estimated price of electricity (€/MWh)
C_t: Total annual cost (in this case it is the annual operation and maintenance cost (€M))
k: Discount rate or interest rate.

The IRR is defined as the interest rate that the project is expected to have if there were no profit or loss. The higher the IRR, the higher the return on investment. The IRR has been calculated using equation (7).

$$0 = -C_i + \sum_{t=1}^{n} \frac{F_t}{(1+TIR)^t} \tag{7}$$

The PAYBACK is the year in which the sum of updated cash flows equals the initial investment cost.

The total benefit is defined as the NPV divided by the total cost (investment cost plus total O&M cost) in percentage. It has been calculated using equations (8) and (9).

$$B = \frac{NPV}{C_T} \times 100 = \frac{NPV}{C_i + C_{O\&M}} \times 100 \tag{8}$$

$$C_{O\&M} = \sum_{t=1}^{n} \frac{C_t}{(1+k)^t} \tag{9}$$

Where:

B: Total profit in percentage terms (%)
C_T: Current total cost of the installation throughout its lifetime (€ M)
$C_{(O\&M)}$: Current total O&M cost during the lifetime of the installation (M €)

The annualized benefit refers to the profit of the periods when the initial investment has already been amortized. It has been calculated using equation (10).

$$B_a = \frac{10^6 \times VAN}{(n - Payback) \times 1000 P_i} \tag{10}$$

Where:

B_a: annualized benefit (€/kW·año)

The parameters used to do the calculations are the followings:

p_u: 1000 €/MW
n: 25 years
p_{ue}: 135 €/MWh (first 4 years) and 55 €/MWh (remaining years)

Annualized O&M cost (C_t): 1,5% of total initial investment.

k: 2%

Justification of the values selected:
Average PV facilities (including installation and commissioning costs) in the Canary Islands are currently a bit above 1000 €/MW for small/medium size facilities, but they are expected to continue decreasing to a value close to 1000 €/MW within next years.

Common values for lifetime of PV facilities found in the literature are between 20 and 30 years. An average lifetime has been selected.

The price of electricity has been estimated based on current and projected electricity prices. Currently spot market electricity prices in Spain are very high and, thus, PV is paid on average over 200 €/MWh. The high spot market electricity prices in Spain are expected to last for the next, at least, four years and then to decrease to prices similar to previous years. Being rather conservative, the forecasted spot market electricity prices for PV were estimated in 135 €/MWh for the first 4 years after commissioning and 55 €/MWh for the remaining years [40,41]. In fact, market prices paid to PV facilities in 2021 reached peaks as high as 400 €/MWh. The average price paid to PV facilities in 2021 was over 120 €/MWh and the average price paid to PV facilities in the last 3 months of 2021 was around 200 €/MWh [42].

2.7.3. Additional benefits

The integration of solar photovoltaic in open parking spaces and on water deposits offer several additional benefits besides the electricity production. Additional benefits depend on type of intervention, whether open parking spaces or water deposits. Open parking spaces covered by PV will provide several benefits as shading the cars and, thus, avoiding their excessive heating which cause discomfort for car drivers. In the case of open water deposits covered by PV, the PV system will hinder water evapotranspiration losses, which are, later on, translated into economical losses, thus providing an extra economic benefit.

3. Results

3.1. Solar radiation

3.1.1. Solar radiation data

In total, 63 pyranometers were used to check the data from the two maps selected for the Canary Islands. Since the Canary Islands has a total area of 7493 km2, this means an average of 1 pyranometer per 119 km2. Therefore, the pyranometer network used to verify the maps is quite dense. The longest data series are those from AEMET (Spanish Meteorological Agency) and SIAR (Agro-climatic Information System for Irrigation). The AEMET series of 4 consecutive years from 7 different meteorological stations were used. The climatological data from AEMET can be consulted in Ref. [43], which include hourly solar radiation series of many decades. The Ministry of Agriculture, Fisheries, Food and Environment also makes their climatological data, collected through the Agrometeorological Stations Network of the SiAR (Agro-climatic Information System for Irrigation), available via web [44]. This web system provides meteorological data every 30 min, hourly, daily, weekly and/or monthly from 395 stations distributed throughout Spain, which have been collecting global solar irradiation data on the horizontal plane since 2004. Data series of the 20 SIAR stations located in the Canary Islands from two consecutive years were used. Series of minute data from 9 consecutive years provided by the Astrophysics Institute of the Canary Islands for the island of La Palma were also used to check map data. In addition to sources from public agencies, data from private developers at two locations were also used.

To achieve the highest possible quality of data in different locations, an extensive bibliographic search of average solar radiation data was also carried out. It is worth highlighting the data on annual averages of solar radiation that could be obtained from the Bioclimatic Map of the Canary Islands [45], which provides data for specific locations in the Canary Islands; 13 of them were used for different locations on the islands.

3.1.1.1. Comparison between the GRASS-r.sun model and pyranometer data. The annual average data from the 63 pyranometer were compared to the solar annual radiation data from GRASS-r.sun. Results show that there is no correlation between the annual average of the r-sun model and the annual average from the pyranometer, beyond the expected result that the GRASS-r.sun mean is higher, since it is based on a clear sky model. But no consistency is observed beyond that, the differences varied from 5% to more than 50%. Therefore, the data from the GRASS-r.sun model will not be used in this work. These large differences may be due to many circumstances, e.g. the numerous microclimates that are identified on the islands as well as the abrupt orography of most of the Canary Islands, factors that condition significant solar radiation changes over relatively short distances.

3.1.1.2. Comparison between the solar radiation map of the Canary Islands and pyranometer data. Table 2 shows the results of comparing the solar radiation map of the Canary Islands with the pyranometer data for 63 locations. Table 2 shows the Mean Absolute Percentage Error (MAPE) and the Root Mean Squared Error (RMSE). The cells in grey show MAPE values over 10%; 13 values in total. All these values correspond to locations in Tenerife except for 3 of them (locations 44, 46 and 50). Overall, the differences are not consistent (sometimes downwards and others upwards) but, in most cases, they are not significant, except in the case of Tenerife, where the data from the Solar Map consistently provide lower values than those recorded by pyranometers. Thus, it has been decided to consider the Solar Map data as an adequate data source for all the islands except for Tenerife. On the island of Tenerife, the Solar Map data have been weighted upwards using the mean of the deviations observed in all measurement stations except for the Izaña one, which showed a very large deviation, but it was not considered meaningful since it is located in a National Park where no photovoltaic installation is foreseen.

Table 3 shows different statistical parameters for the above mentioned locations: MAE, weighted MAPE, RSME, correlation coefficient, Mean Bias Error (MBE) and Mean Bias Percent Error (MBPE); for three different cases. The first case is the average value for the 63 above mentioned locations. The second one is the average value for all above mentioned locations except for the 9 Tenerife locations. The third one includes all 63 locations but in this case the radiation map values for the locations in Tenerife were increased 10%. As it can be observed, the statistical parameters improve when Tenerife is excluded and they improve even more when the modified values for Tenerife are included. For example, the average weighted MAPE for all original 63 locations is 6.1%, while this value comes down to 4.8% when the Tenerife locations

Table 2
Comparison between pyranometer data and the Solar Radiation Map of the Canary Islands.

Location	Solar radiation pyranometer (Wh/m2·d)	Solar Radiation Map (Wh/m2·d)	MAPE	RMSE
1. Maspalomas	5531	5455	1.37%	76
2. Roque de los Muchachos	5810	6072	−4.51%	262
3. Aeropuerto FTV	5765	5466	5.18%	299
4. Aeropuerto GC	5650	5331	5.65%	319
5. Aeropuerto LZT	5453	4994	8.41%	459
6. Izaña	6818	5252	22.97%	1566
7. Sta Cruz Tenerife	5593	4397	21.39%	1196
8. Aeropuerto TNF norte	5240	4590	12.41%	650
9. Aeropuerto TNF sur	5751	4863	15.44%	888
10. Valverde	4300	4556	−5.95%	256
11. La Restinga	5600	5498	1.82%	102
12. San Sebastián	5600	5712	−2.00%	112
13. Valle Gran Rey	5100	5024	1.49%	76
14. Llanos de Aridane	5200	5163	0.71%	37
15. Santa Cruz de La Palma	4500	4789	−6.42%	289
16. Granadilla	5300	4812	9.21%	488
17. Puerto Santiago	5300	4960	6.42%	340
18. La Laguna	5000	4674	6.52%	326
19. Puerto de la Cruz	4500	4134	8.13%	366
20. Santa Cruz de Tenerife	5100	4466	12.43%	634
21. Las Palmas GC	4700	4842	−3.02%	142
22. Santa Lucía de Tirajana	5700	5818	−2.07%	118
23. La Aldea de San Nicolás	5800	5744	0.97%	56
24. San Fernando de Maspalomas	5200	5459	−4.98%	259
25. Mogán	5200	5517	−6.10%	317
26. Santa Brígida	4700	4923	−4.74%	223
27. Sardina de Gáldar	5100	5193	−1.82%	93
28. Cañadas del Río	5700	5780	−1.40%	80
29. El Cotillo	5600	5734	−2.39%	134
30. Betancuria	5500	5763	−4.78%	263
31. Janubio	5300	5272	0.53%	28
32. Los Valles	5400	5483	−1.54%	83
33. Frontera	4964	5117	−3.08%	153
34. Antigua - pozo negro	5396	5443	−0.88%	47
35. Antigua - molino de agua	5551	5534	0.31%	17
36. Arucas	4435	4539	−2.34%	104
37. Gáldar	4720	4890	−3.61%	170
38. San mateo	4918	5204	−5.82%	286
39. La Aldea	5630	5804	−3.10%	174
40. Vecindario	5699	5698	0.01%	1
41. Hermigua	4133	4166	−0.80%	33
42. San Sebastián de La Gomera	5343	5383	−0.75%	40
43. Barlovento	4195	4443	−5.90%	248
44. Fuencaliente	3979	4388	−10.27%	409
45. Los Llanos de Aridane	5148	5165	−0.32%	17
46. Los Llanos de Aridane II	5825	5167	11.29%	658
47. Puntallana	4816	4956	−2.90%	140
48. Tazacorte	5259	5237	0.42%	22
49. El Socorro	4445	4856	−9.24%	411
50. La Degollada	4104	5259	−28.14%	1155
51. La Torrecilla	5345	5224	2.26%	121
52. Haría	5213	5221	−0.14%	8
53. Masdache	5399	5106	5.43%	293
54. Tinajo	4782	4864	−1.72%	82
55. Guía de Isora	5529	4960	10.29%	569
56. Garimba	4593	4112	10.47%	481
57. Buenavista del Norte	4630	4224	8.77%	406
58. La Laguna - Güimar	5479	4564	16.70%	915
59. Las Galletas	4952	4146	16.28%	806
60. Puerto de la Cruz	4284	4026	6.01%	258
61. Valle Guerra - Isamar	4742	4146	12.56%	596
62. Valle Guerra - Pajarillos	4684	4274	8.75%	410
63. El Pico	4321	4238	1.92%	83

are excluded and it comes down again to 4.1% when the modified values for Tenerife are included. Thus, it can be concluded that the radiation map are acceptable if the values for Tenerife island are increased by 10%.

3.2. Shadow factor

The methodology used to calculate the shadow factors (SF), as described in the previous section, resulted in SF values that varied from enclosure to enclosure but, in general, the range of the calculated values did not vary significantly. In total, 2501 uncovered parking spaces and a 1602 water deposits were analysed. There variations by type of surfaces (parking or deposits) are not very large, although there are differences. So, the mean shadow factor in deposits is 0.024 (2.4%) and the mean shadow factor in parking spaces is 0.036 (3.6%). This difference is due to the fact that large

Table 3
Statistical parameters: comparison pyranometer data vs Solar Radiation Map.

	MAE	MAPE weighted	RSME	Correlation Coefficient	MBE	MBPE (Bias)
1. Average value	311.88	6.07%	443.41	0.678	118.03	1.93%
2. Average value without Tenerife	192.67	4.80%	278.52	0.857	−78.73	−1.89%
3. Average value (with 10% increase in Tenerife)	211.07	4.11%	307.68	0.824	−12.25	−0.64%

deposits are generally located in places with fewer objects around them (thus, fewer shadows) than the urban surroundings that are found around most parking spaces.

Regarding the seasonal differences, they are not significant either, but they do confirm the larger shadow projections over the winter season. The average of the 2501 uncovered parking spaces analysed showed the following shadow factor values: 2.95% (day 80), 2.43% (day 172), 2.91% (day 264) and 6.17% (day 355). These values clearly show the larger shadow effect over winter (more than double than in any other season of the year), the rest of the representative values of the different seasons are very similar to each other with practically the same average over spring and autumn and less shadow projections over summer. The mean of the 1602 deposits analysed show the following shadow factor values: 1.9% (day 80), 1.43% (day 172), 1.88% (day 264) and 4.4% (day 355). These values clearly show the larger shadow effect over winter (more than double than in any other season of the year), the rest of the representative values of the different seasons are very similar to each other with practically the same average over spring and autumn and less shadow projections over summer. These values in winter, a season in which the shadow factor more than doubled the yearly average value, reflect the larger projection of shadows in this season due to the lower position of the sun. Likewise, it can be observed that the values of the shadow factors are significantly lower in deposits than in parking spaces along the whole year.

Table 4 shows an example of the calculation of the shadow factor including the following data (from left to right): island, municipality, water deposit area (m^2), radiation ratio between the two results from r.sun tool (with and without object above the ground level) for 4 days of the year (representative of each season) and their annual mean. This last value is the representative one for the shadow factor (FS) and the one that has been used as such for calculation purposes.

3.3. Available area, power and annual energy production for deposits and parking spaces

Table 5 shows the results for the parking areas and water deposits: the available areas identified on each island, the resulting power and the annual production (calculated with the equations set described in the previous section) and the corresponding utilization and shadow factors.

As shown in Table 5, the area of the uncovered parking areas is much larger than the deposits' area, represents ca. 30% of the total area (2 km^2 of water deposits) compared to ca. 5 km2 of uncovered parking spaces. However, in terms of power and production the water deposits represent around 45%, this is due to the fact that fewer shadows are projected on the water deposits than on the parking spaces, which are more exposed to the shadows created by the urban surroundings. The total power reaches 502 MW and the production 787 GWh/a.

3.4. Photovoltaic energy production

The hourly and monthly PV productions have been calculated. Results are shown for two of the islands, Gran Canaria and La Palma. Gran Canaria is the island that shows the highest PV production in absolute terms and a similar PV production contribution as the regional one. La Palma is that shows the highest average PV contribution to the annual electricity demand, around 41%.

3.4.1. Hourly photovoltaic production in Gran Canaria

Fig. 8 shows the results of the hourly photovoltaic production in comparison to the hourly electricity demand for the island of Gran Canaria, the yearly average PV contribution is 8% although there are peaks that can reach values as high as 40%. Fig. 9 shows a zoom of Fig. 8 for the month of May, where one 40% PV contribution peak the 26th of May can be observed. Fig. 10 shows the PV contribution to the hourly electricity demand in Gran Canaria. As it can be observed the highest peak contributions are found in the months of April and May. Fig. 11 shows the PV contribution to the hourly electricity demand in Gran Canaria aggregated by ranges, showing the number of hours per year within each range. The highest range, 30–40% PV contribution, shows a relatively small number of hours, 121 h.

3.4.2. Monthly photovoltaic production in Gran Canaria

Fig. 12 shows the monthly PV contribution in comparison to the monthly electricity demand in Gran Canaria. It can be observed that the months that show the highest PV contribution are May and June. Although the months that show the highest PV production in absolute terms are May and July. All in all, from April to August the monthly PV contribution is very similar in absolute terms as well as in percentage terms.

3.4.3. Hourly photovoltaic production in La Palma

Fig. 13 shows the results of the hourly photovoltaic production in comparison to the hourly electricity demand for the island of La Palma, the yearly average PV contribution is 41% although there are peaks that can reach values as high as 191%. Fig. 14 shows a zoom of Fig. 13 for the month of May, where one 190% PV contribution peaks can be observed. Fig. 15 shows the PV contribution to the hourly electricity demand in La Palma. As it can be observed the highest peak contributions are found in the month of May, although from March to October peaks over 100% can be observed. This high PV contribution leads to a cumulative storage need of 12.52 GWh/a, 11.7% of the PV production need to be stored, which represent ca. 5% of the annual demand. Fig. 16 shows the PV contribution to the hourly electricity demand in La Palma aggregated by ranges, showing the number of hours per year within each range. The highest range, over 100% PV contribution, shows the highest number of hours (except for the night hours), 1469 h.

3.4.4. Monthly photovoltaic production in La Palma

Fig. 17 shows the monthly PV contribution in comparison to the monthly electricity demand in La Palma. It can be observed that the months that show the highest PV contribution is July, which also shows the highest PV production in absolute terms. All in all, from April to August the monthly PV contribution is very similar in absolute terms as well as in percentage terms.

Table 4
Calculation of the shadow factor for a selection of water deposits.

Island	Municipality	Area (m2)	Radiation (day 80)	Radiation (day 172)	Radiation (day 264)	Radiation (day 355)	SF_mean
LA GOMERA	AGULO	47567	0.9919	0.9944	0.9920	0.9837	0.991
LA GOMERA	VALLEHERMOSO	37475	0.9816	0.9890	0.9819	0.9620	0.979
LA GOMERA	SAN SEBASTIÁN DE LA GOMERA	3037	0.9913	0.9814	0.9913	0.9917	0.989
LA GOMERA	HERMIGUA	21057	0.9760	0.9951	0.9770	0.9363	0.971
LA GOMERA	AGULO	8614	0.9947	0.9962	0.9939	0.9809	0.991
LA GOMERA	VALLEHERMOSO	11347	0.9988	0.9981	0.9989	0.9954	0.998
LA GOMERA	SAN SEBASTIÁN DE LA GOMERA	3753	0.9867	0.9927	0.9858	0.9764	0.985
LA GOMERA	ALAJERÓ	6227	0.9898	0.9920	0.9907	0.9689	0.985
LA GOMERA	SAN SEBASTIÁN DE LA GOMERA	779	0.9913	0.9948	0.9888	0.9437	0.98
LA GOMERA	VALLE GRAN REY	1068	0.9836	0.9857	0.9828	0.9675	0.98
LA GOMERA	ALAJERÓ	5876	0.9981	0.9986	0.9983	0.9968	0.998
LA GOMERA	VALLEHERMOSO	4504	0.9969	0.9980	0.9971	0.9969	0.997
LA GOMERA	HERMIGUA	6589	0.9059	0.9169	0.9077	1.0000	0.933
LA GOMERA	VALLEHERMOSO	4591	0.9445	0.9611	0.9457	0.8248	0.919
LA GOMERA	SAN SEBASTIÁN DE LA GOMERA	1864	0.8650	0.9306	0.8679	0.7372	0.85
LA GOMERA	VALLEHERMOSO	2671	0.9771	0.9839	0.9779	0.9617	0.975
LA GOMERA	SAN SEBASTIÁN DE LA GOMERA	1297	0.9422	0.9728	0.9439	0.8744	0.933
LA GOMERA	AGULO	1110	0.9443	0.9719	0.9484	0.7795	0.911
LA GOMERA	AGULO	1962	0.8856	0.9111	0.8867	0.7906	0.869
LA GOMERA	VALLEHERMOSO	1629	0.9617	0.9774	0.9635	0.8591	0.94
LA GOMERA	HERMIGUA	1485	0.9656	0.9580	0.9644	0.9041	0.948
LA GOMERA	HERMIGUA	2110	0.9219	0.9848	0.9229	0.9090	0.935
LA GOMERA	VALLE GRAN REY	1585	0.9987	0.9972	0.9985	0.9939	0.997
LA GOMERA	VALLE GRAN REY	927	0.9971	0.9974	0.9970	0.9962	0.997
LA GOMERA	AGULO	867	0.9641	0.9875	0.9775	0.8552	0.946

Table 5
Area, power and yearly energy production of parking areas and water deposits.

		Area (m2)	Power (kW)	Production (MWh/a)
EL HIERRO	Parking	56,475	4000	6010
	Water tank	8137	659	1027
FUERTE-VENTURA	Parking	615,727	43,611	76,117
	Water tank	92,666	7501	13,135
GRAN CANARIA	Parking	1,629,281	115,399	183,348
	Water tank	830,406	67,218	104,544
LA GOMERA	Parking	76,084	5389	8792
	Water tank	18,434	1492	2307
LA PALMA	Parking	168,957	11,967	18,471
	Water tank	690,987	55,933	88,835
TENERIFE	Parking	1,836,851	130,100	191,887
	Water tank	227,970	18,453	27,216
TOTAL	Parking	**4,882,210**	**345,797**	**541,451**
	Water tank	**1,933,374**	**156,499**	**245,559**

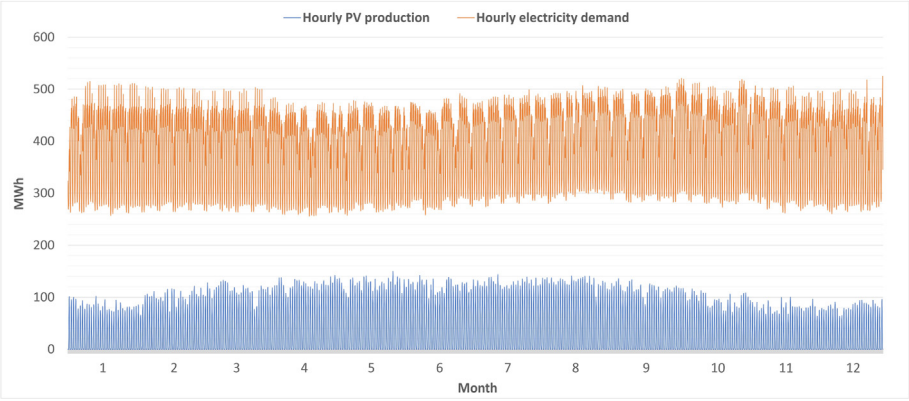

Fig. 8. Hourly PV production versus electricity demand (Gran Canaria).

3.4.5. Annual photovoltaic production and energy demand supplied by photovoltaic

Table 6 shows the summary of the annual photovoltaic production of the elements identified in this study (parking spaces and water deposits) compared to the electricity demand in 2019.

Table 6 shows that the percentage of photovoltaic production in parking spaces is much higher than in water deposits, except on the island of La Palma, which has an exceptionally high PV contribution

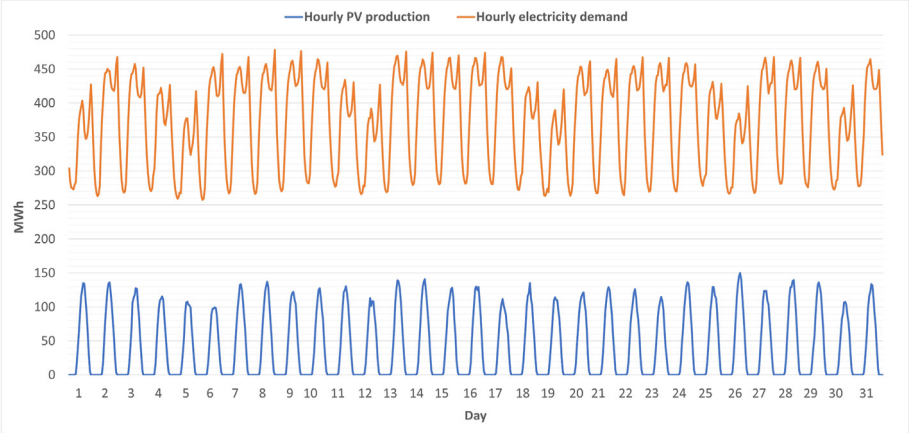

Fig. 9. Hourly PV production versus electricity demand for the month of May (Gran Canaria).

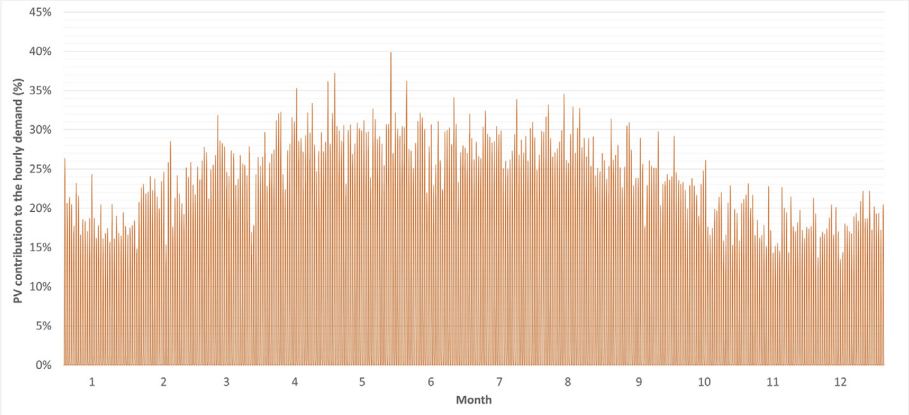

Fig. 10. PV contribution to the hourly electricity demand (Gran Canaria).

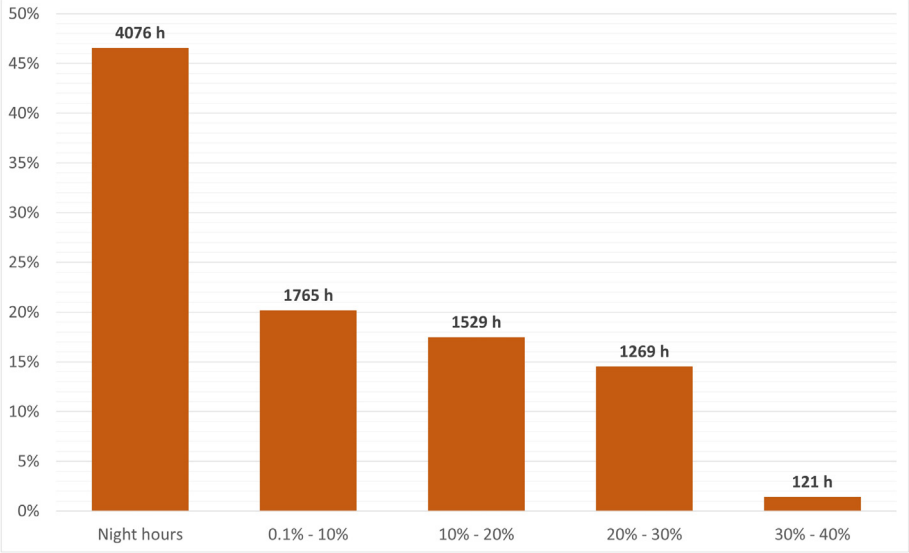

Fig. 11. PV contribution to the hourly electricity demand aggregated by ranges (Gran Canaria).

from water deposits. The percentages of electricity demand supplied by PV (global and also per element), vary significantly from island to island. Nonetheless, in general terms, it can be concluded that the percentage of demand supplied by photovoltaic solar energy using only uncovered parking spaces and water deposits ranges from 6% to 14% (an average of ca. 9%). This is the case for all the islands except for the island of La Palma, where this percentage raises until 41%, mainly due to the big area covered by water

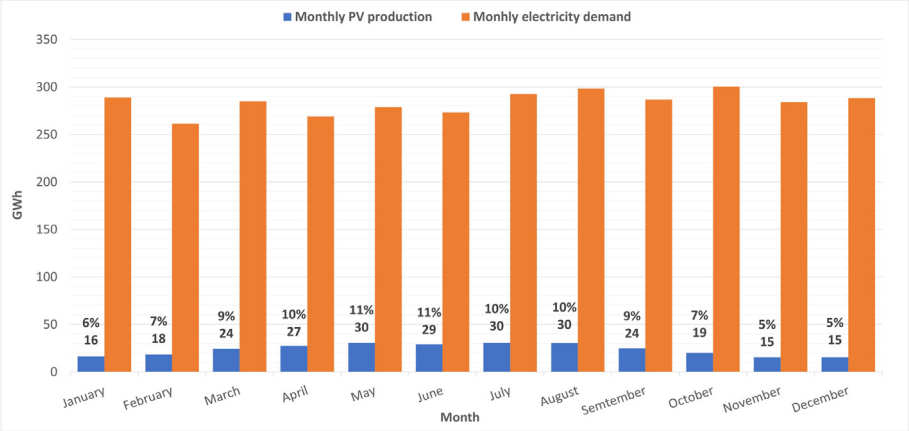

Fig. 12. PV contribution to the monthly electricity demand (Gran Canaria).

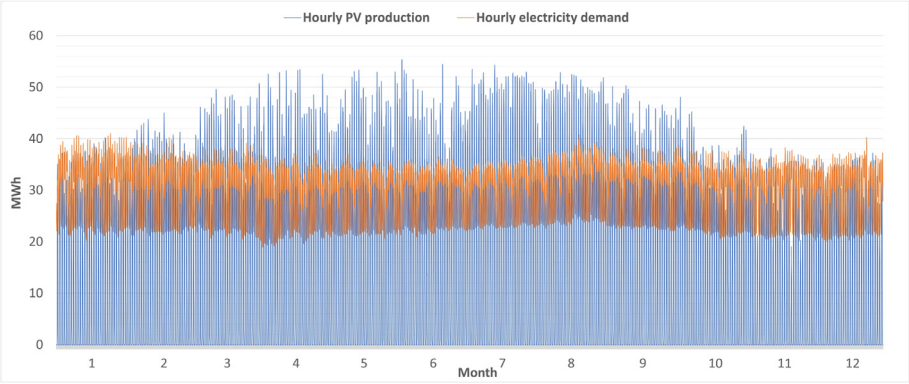

Fig. 13. Hourly PV production versus electricity demand (La Palma).

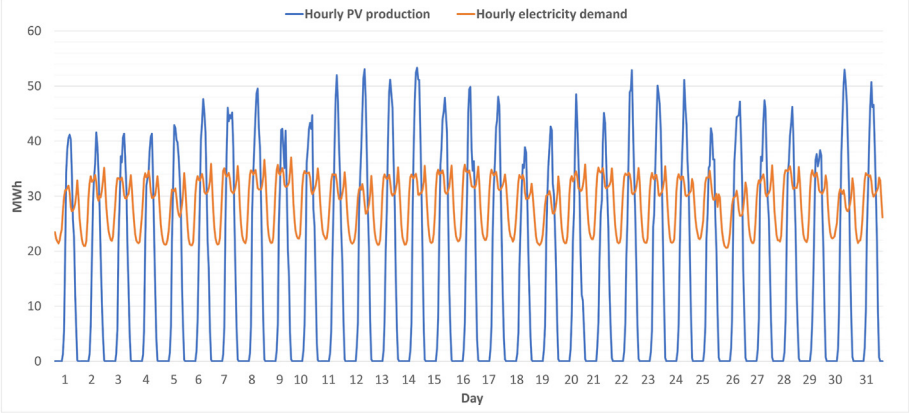

Fig. 14. Hourly PV production versus electricity demand for the month of May (La Palma).

deposits on this island.

3.5. Impact of the photovoltaic production at island level and additional benefits of the proposed solution

This section summarizes the results of the impact of the proposed solutions.

3.5.1. Impact of the photovoltaic production at island level

Table 7 shows the resulting PV surface that can be installed on parking spaces and water deposits as well the percentage of the annual insular demand that could be supplied by photovoltaic energy, contextualised for each island, indicating also the total surface, total population and per capita electricity consumption, in order to estimate the real impact of the proposed solutions at the island level.

The annual average demand growth has been calculated as the average growth of the last 5 years. The resident population refers to the population that permanently lives on the islands and their residence is fixed on the islands. The floating population refers

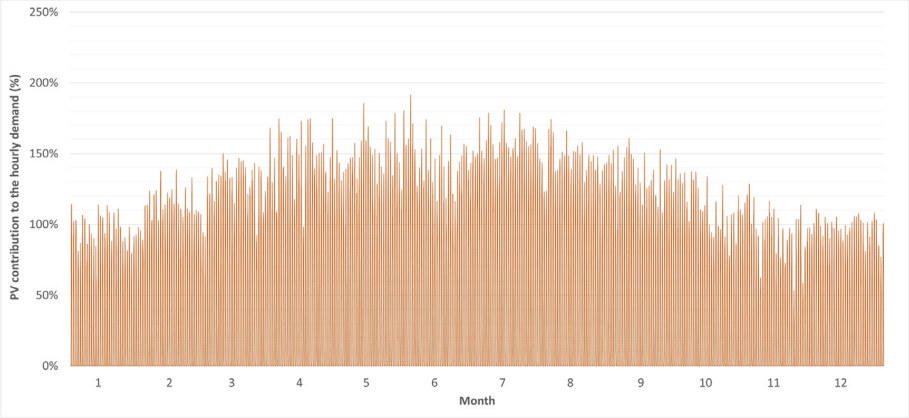

Fig. 15. PV contribution to the hourly electricity demand (La Palma).

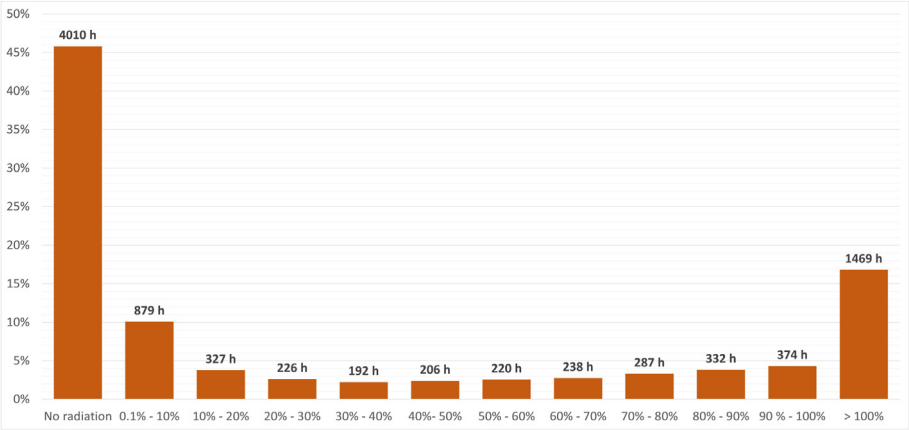

Fig. 16. PV contribution to the hourly electricity demand aggregated by ranges (La Palma).

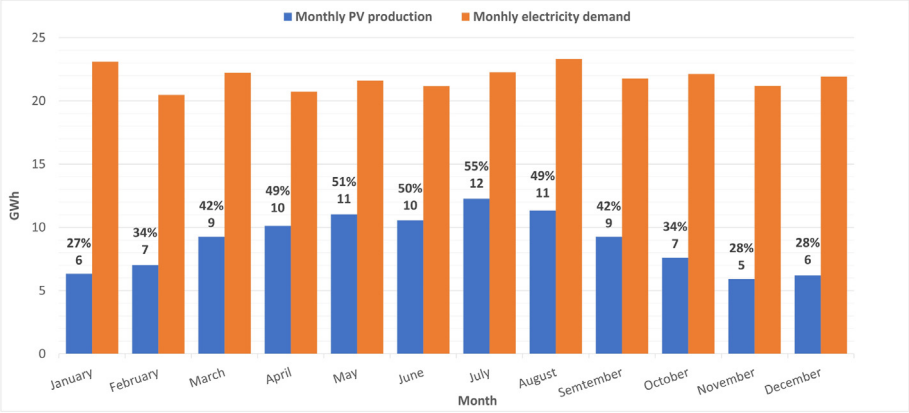

Fig. 17. PV contribution to the monthly electricity demand (La Palma).

mainly to the tourists, including those that spend many months on the islands but their residence is located in a foreign country.

The average annual PV contribution is significantly different from island to island as, thus, their potential contribution to the island' energy plan. In this regard, the PV contribution of open parking spaces and water deposits shows their lowest percentage in the island of Tenerife, where this contribution is as low as 6.2%. Thus, in order to reach the required 100% RES in 2040, it is recommended to significantly increase the PV contribution by adding other PV actions such as e.g. PV roofs or PV greenhouses. At the other end, the island of La Palma, where this contribution is as high as 41%. Nearly no additional PV contribution would be needed to reach the required 100% RES in 2040, since this contribution already means nearly 12% PV storage needs. Although there could be some complementarity with PV roofs, the main complementarity should come from wind energy and other RES sources in

Table 6
Annual photovoltaic production compared to the electricity demand in 2019.

		Production (GWh/a)	% of electricity demand supplied by PV (2019)	Electricity Demand 2019 (GWh)
EL HIERRO	Parking	6.0	9.7%	
	Water deposit	1.0	1.7%	
	TOTAL	7.0	11.4%	62
FUERTE-VENTURA	Parking	76.1	10.6%	
	Water deposit	13.1	1.8%	
	TOTAL	89.2	12.4%	717
GRAN CANARIA	Parking	183.3	5.1%	
	Water deposit	104.5	2.9%	
	TOTAL	287.8	8.0%	3582
LA GOMERA	Parking	8.8	11.4%	
	Water deposit	2.3	3.0%	
	TOTAL	11.1	14.4%	77
LA PALMA	Parking	18.5	7.1%	
	Water deposit	88.8	33.9%	
	TOTAL	107.3	41%	281
LANZAROTE	Parking	56.8	6.3%	
	Water deposit	8.5	0.9%	
	TOTAL	65.3	7.2%	906
TENERIFE	Parking	191.9	5.2%	
	Water deposit	27.2	0.7%	
	TOTAL	219.1	5.9%	3711
CANARY ISLANDS	Parking	541.4	6.10%	
	Water deposit	245.4	2.77%	
	TOTAL	786.8	8.87%	8874

Table 7
Annual photovoltaic production and main parameters for each island.

	Island' surface (km2)	Resident Population (2019)	Floating population (2019)	Total population (2019)	Electricity Demand 2019 (GWh)	Average annual demand growth	Yearly electricity demand per capita (MWh/a·hab)	PV production GWh/a (deposits and parkings)	PV Contri-bution %
Lanzarote	875	154,530	65,007	219,537	861	1.36%	3.9	65.3	7.6%
Fuerte-ventura	1659	126,227	45,231	171,458	683	1.64%	4.0	89.2	13.1%
Gran Canaria	1560	870,595	85,921	956,516	3406	0.23%	3.6	287.8	8.5%
Tenerife	2034	966,354	110,622	1,076,976	3547	0.56%	3.3	219.1	6.2%
La Palma	708	85,840	6214	92,054	262	1.06%	2.8	107.3	41.0%
La Gomera	370	22,426	1679	24,105	74	1.66%	3.1	11.1	15.0%
El Hierro	269	11,338	78	11,416	43	−0.03%	3.8	7	16.3%
TOTAL	7475	2,237,310	314,752	2,552,062	8875	**0.60%**	3.5	786.8	8.9%

order to decrease storage needs. For the rest of the islands, the PV contribution ranges from 7.6% to 16.3%. Thus, some increase in the PV contribution by adding other PV actions such as PV roofs are still recommended, although the main complementary contribution should also come from other RES sources.

3.5.2. Economic analysis of the proposed solutions

Table 8 summarizes the results of the economic analysis for each of the islands, including the installed power per island and the yearly production (calculated in previous section) to be able to calculate the normalized production per MW installed, the NPV per MW, the yearly net profit per installed MW after amortization (it has been supposed that benefits will be rip after the amortization period), the net profit as percentage of the total investment, the IRR and the payback.

As shown in Table 8 the payback time depends on the island but it is always located between 6 and 9 years (best and worst case scenarios). The island that show the best payback time is Fuerte-ventura and the island that show the worst one is Tenerife, mainly because many of the installations are located in the northern part of the island, which shows lower radiation data. All in all, the yearly net profits per MW installed ranges from 48,000 € to 61,000 € and the IRR varies from 10% to 13%.

3.5.3. Additional benefits of the proposed solutions

Additional benefits could also be translated into economic

Table 8
Economic analysis for each island.

	Gran Canaria	Tenerife	Lanzarote	Fuerte-ventura	La Palma	La Gomera	El Hierro
Installed Power (MW)	183	149	40	51	68	7	5
Yearly Production (MWh/a)	287,892	219,103	65,300	89,252	107,306	11,099	7037
Production per MW installed (MWh/MW)	1576	1475	1622	1746	1580	1613	1510
NPV (k€/MW)	917	775	982	1156	923	969	825
Yearly net profit (k€/MW·a)	52	48	55	61	53	54	50
Net benefit	71%	64%	76%	89%	71%	75%	64%
IRR	11%	10%	12%	13%	11%	11%	10%
Payback (years)	7.5	9	7	6	7.5	7	8.5

benefit. In the case of the open parking spaces, a side effect of the PV systems is the shading of the cars, which will reduce the discomfort for car drivers due to excessive car heating; this effect could be monetized. In the case of open water deposits, water evapotranspiration losses could be as high as 5–10%. PV systems will reduce these losses, thus providing an extra economic benefit.

4. Conclusions

This study shows the important potential of photovoltaic solar energy and the development that could be achieved without using additional land as, in this case, by using uncovered parking spaces and large water deposits. It is important to highlight that it is key to work with high quality solar radiation data to be able to make a good estimate of the photovoltaic production. In this research the methodology proposed is to calibrate the selected solar maps with a network pyranometers that should be as large as possible. The network used in this work consisted in 63 pyranometers (approximately 1 pyranometer per 120 km2). By comparing the selected maps with the network of pyranometers, it can be concluded that no correlation was found with the GRASS-r.sun model, probably due to the numerous microclimates that are identified on the islands as well as their abrupt orography. The comparison with the Solar Map of the Canary Islands provided better results, the differences were not significant except for one of the islands, whose values were consistently lower than those recorded by the pyranometers. Therefore, it was decided to weight the Solar Map data for this island (according to the pyranometer data), and to use directly the Solar Map data for the rest of the islands.

In regard to the methodology implemented there are two main novelties in comparison to the literature review. On one hand, to estimate the available parking and deposit surfaces suitable for PV exploitation, one novelty is the use of certain layers from topographic and cartographic regional maps and certain orthophoto photointerpretation techniques. On the other hand, the determination of the shadow factor was estimated using a novel technique which combines the use of LIDAR and the r.sun software tool. The first step consisted in the generation of the digital terrain models from the information of the LIDAR points. Two models were generated, one digital surface model that includes all the elements above the terrain (buildings, trees …) and a second digital terrain model without the objects on top of the ground. The r.sun tool was run for each of the enclosures twice, once for each of the two models, and the irradiation was calculated for 4 selected days of the year in each case.

Results show that the photovoltaic solar energy that can be installed on open air parking spaces and large water deposits could supply an important part of the energy demand. The total installable power reaches 502 MW, the production 787 GWh/a, which contributes to cover nearly 9% of the annual regional electricity demand (6% on parking spaces and nearly 3% on water deposits), although this percentage varies largely from island to island, this contribution was as high as 38% in the island of La Palma. Although the average annual contribution is well below 100%, the hourly analysis shows that the hourly contributions can be very high. In Gran Canaria, where the annual average contribution was 8%, one can find hourly PV contributions as high as 40%. In La Palma, where the annual average contribution was 38%, one can find nearly 1500 h when the hourly PV contributions is higher than 100%. The monthly contribution is more evenly distributed, ranging in the case of Gran Canaria from 5% to 11% and in the case of La Palma from 27% to 55%.

In general, the typology of surface that contributes the most, in terms of power and annual production, is the uncovered parking spaces, mainly due to the fact that the total parking area is generally much larger than that of the water deposits area. Nonetheless, this distribution is uneven among the different islands, and even in one of the islands the contribution of the water deposits is higher than the one from the parking spaces. Regarding the shadow factors, they are similar in both cases, reaching around 2.4% in the case of water deposits and 3.5% in the case of uncovered parking spaces. This higher shadow coefficient in the case of parking spaces is mainly due to the larger shadows projected on urban areas, which affect parking spaces more than water deposits. The seasonal analysis of the shadow factors showed similar values throughout the year except for winter (whose values more than double the values from any other season). This result reflects the larger shadow projection during this season due to the fact that the sun is lower.

The estimated utilization factor is 35% for parking spaces and 40% for water deposits. Thus, as per shadow factor as well as by utilization factor, the water deposits result in a higher ratio of installable power per surface unit: on average 33.7% of the parking area can be covered with photovoltaic panels compared to 39.2% in the case of water deposits. However, the area of uncovered parking spaces that has been identified is, in general, much larger than that of water deposits (in total, about 5 km2 of surface of uncovered parking spaces compared to about 2 km2 of water deposits), thus the power that can be installed in parking areas is higher than on water deposits, although the useable surface per unit area is higher in the water deposits.

The economic analysis of the PV facilities shows good results with payback time that varied from 6 to 9 years depending on the island.

CRediT authorship contribution statement

Schallenberg-Rodriguez Julieta: Conceptualization, Methodology, Data processing (solar radiation), Writing – original draft, Investigation, Calculations (PV power and production), Supervision, Visualization, Project administration, Writing – review & editing. **Rodrigo-Bello José-Julio:** Software, processing, Geographical Information System (GIS), cartographic and topographic information, r-sun GRASS, identification of suitable areas. **Yanez-Rosales Pablo:** Calculation of hourly and monthly PV production; economic calculations, statistical metrics.

Declaration of competing interest

The authors declare that they have no known competing financial interests or personal relationships that could have appeared to influence the work reported in this paper.

Acknowledgment

This research work has been financed by GRAFCAN.

References

[1] M.C. Brito, N. Gomes, T. Santos, J.A. Tenedó Rio, Photovoltaic potential in a Lisbon suburb using LiDAR data, Sol. Energy 86 (1) (2012) 283–288, https://doi.org/10.1016/j.solener.2011.09.031. Elsevier.
[2] S. Castellanos, D.A. Sunter, D.M. Kammen, Rooftop solar photovoltaic potential in cities: how scalable are assessment approaches? Environ. Res. Lett. 12 (12) (2017) 125005, https://doi.org/10.1088/1748-9326/aa7857.
[3] M. Mangiante, P. Whung, L. at al. Zhou, et al., Economic and Technical Assessment of Rooftop Solar Photovoltaic Potential in Brownsville, Texas, US. Computers, Environment and Urban Systems 80, Elsevier, 2020, p. 101450.
[4] Song X, Huang Y, Zhao C, Liu Y, Lu Y, Chang Y, et al. An approach for estimating solar photovoltaic potential based on rooftop retrieval from remote sensing images. MdpiCom n.d. doi:10.3390/en11113172.
[5] L.R. Rodríguez, E. Duminil, J.S Ramos, U. Eicker, Assessment of the photovoltaic potential at urban level based on 3D city models: a case study and new methodological approach, Sol. Energy 146 (2017) 264–275. Elsevier.

[6] A. Tiwari, I.A. Meir, A. Karnieli, Object-based image procedures for assessing the solar energy photovoltaic potential of heterogeneous rooftops using airborne LiDAR and orthophoto, Rem. Sens. 12 (2020), https://doi.org/10.3390/rs12020223.
[7] T. Hong, M. Lee, C. Koo, K. Jeong, J.K.-A. Energy, Development of a Method for Estimating the Rooftop Solar Photovoltaic (PV) Potential by Analyzing the Available Rooftop Area Using Hillshade Analysis, Elsevier, 2017.
[8] H. Saadaoui, A. Ghennioui, B. Ikken, Using GIS and photogrammetry for assessing solar photovoltaic potential on Flat Roofs in urban area case of the city of Ben Guerir/Morocco, D-NbInfo (2019), https://doi.org/10.5194/isprs-archives-XLII-4-W12-155-2019.
[9] A. Pinna, L. Massidda, A procedure for complete census estimation of rooftop photovoltaic potential in urban areas, Mdpi (2020), https://doi.org/10.3390/smartcities3030045.
[10] Y. Choi, J. Rayl, C. Tammineedi, J.B.-S. Energy, PV Analyst: Coupling ArcGIS with TRNSYS to Assess Distributed Photovoltaic Potential in Urban Areas, Elsevier, 2011.
[11] N. Luka, S. Seme, D. Zlaus, G. Stumberger, B. Zalik, Buildings Roofs Photovoltaic Potential Assessment Based on LiDAR (Light Detection and Ranging) Data, Elsevier, 2014, https://doi.org/10.1016/j.energy.2013.12.066.
[12] J. Schallenberg-Rodríguez, Photovoltaic techno-economical potential on roofs in regions and islands: the case of the Canary Islands. Methodological review and methodology proposal, Renew. Sustain. Energy Rev. 20 (2013), https://doi.org/10.1016/j.rser.2012.11.078.
[13] J. Schallenberg-Rodriguez, Photovoltaic techno-economical potential on roofs in the Canary Islands, J. Sustain. Dev. Energy, Water Environ. Syst. 2 (2014), https://doi.org/10.13044/j.sdewes.2014.02.0007.
[14] J. Rovisham, S. Doorga, R. Tannoo, · Soonil, D.D.V. Rughooputh, R. Boojhawon, Exploiting the rooftop solar photovoltaic potential of a tropical island state: case of the Mascarene Island of Mauritius, Int. J. Energy Environ. Eng. (2021), https://doi.org/10.1007/s40095-020-00375-9.
[15] M. Boulahia, K.A. Djiar, M. Amado, Combined engineering—statistical method for assessing solar photovoltaic potential on residential rooftops: case of Laghouat in central Southern Algeria, Energies 14 (6) (2021) 1626, https://doi.org/10.3390/en14061626.
[16] Ordóñez J, Jadraque E, Alegre J, Sustainable GM-R. Analysis of the Photovoltaic Solar Energy Capacity of Residential Rooftops in Andalusia (Spain). Elsevier n.d.
[17] D. Assouline, N. Mohajeri, J.L. Scartezzini, Quantifying rooftop photovoltaic solar energy potential: a machine learning approach, Sol. Energy 141 (2010) 278–296. Elsevier.
[18] C. Phillips, R. Elmore, J. Melius, P. Gagnon, R. Margolis, A data mining approach to estimating rooftop photovoltaic potential in the US, J. Appl. Stat. 46 (3) (2019) 385–394, https://doi.org/10.1080/02664763.2018.1492525.
[19] R. Ureña-Sánchez, , Callejón-Ferre ÁJ, J. Pérez-Alonso, Á. Carreño-Ortega, Greenhouse tomato production with electricity generation by roof-mounted flexible solar panels, Sci. Agric. 69 (2012) 233–239, https://doi.org/10.1590/S0103-90162012000400001.
[20] P. Gagnon, R. Margolis, J. Melius, C. Phillips, R. Elmore, Estimating rooftop solar technical potential across the US using a combination of GIS-based methods, lidar data, and statistical modeling, Environ. Res. Lett. 13 (2018), https://doi.org/10.1088/1748-9326/aaa554.
[21] K. Bódis, I. Kougias, A. Jäger-Waldau, et al., A High-Resolution Geospatial Assessment of the Rooftop Solar Photovoltaic Potential in the European Union, Elsevier, 2019.
[22] R. Krishnan, A. Haselhuhn, J.M. Pearce, Technical solar photovoltaic potential of scaled parking lot canopies: A Case Study of Walmart U.S.A, J. Innovat. Sustain. RISUS 8 (2017) 104–125, https://doi.org/10.24212/2179-3565.2017v8i2p104-125.
[23] H.M. Neumann, D. Schär, F. Baumgartner, The potential of photovoltaic carports to cover the energy demand of road passenger transport, Prog. Photovoltaics Res. Appl. 20 (2012) 639–649, https://doi.org/10.1002/pip.1199.
[24] Rigollier C, Bauer O, Wald L, Christelle R, Olivier B, Lucien W. On the Clear Sky Model of the ESRA-European Solar Radiation Atlas with Respect to the Heliosat Method.
[25] K. Scharmer, The European Solar Radiation Atlas: Fundamentals and Maps, 2000.
[26] L. Wald, M. Albuisson, C. Best, C. Delamare, D. Dumortier, E. Gaboardi, et al., SoDa: a Web Service on Solar Radiation, 2004.
[27] L. Wald, M. Albuisson, C. Best, C. Delamare, D. Dumortier, E. Gaboardi, et al., SoDa: a Project for the Integration and Exploitation of Networked Solar Radiation Databases, 2010.
[28] D. Dumortier, M. Fontoynont, SATELLIGHT: A WWW SERVER WHICH PROVIDES HIGH QUALITY DAYLIGHT AND SOLAR RADIATION DATA FOR WESTERN AND CENTRAL EUROPE, 1996.
[29] European Commission, Photovoltaic Geographical Information System (PVGIS) n.D. https://ec.europa.eu/jrc/en/pvgis. (Accessed 6 May 2021).
[30] M. Suri, T. Huld, E. Dunlop, T.C.-I.J. Topics, Geographic Aspects of Photovoltaics in Europe: Contribution of the PVGIS Website, 2008.
[31] E.D. Dunlop, M. Albuisson, L. Wald, et al., Online Data and Tools for Estimation of Solar Electricity in Africa: the PVGIS Approach, 21st European Photovoltaic Solar Energy Conference and Exhibition, 2006, pp. 4–8.
[32] C.T Ian, K.J. Sauer, R.A. Desharnais, Revisiting the model parameters of an existing system using the Photovoltaic System Analysis Toolbox (PVSAT), 2015 IEEE 42nd Photovoltaic Specialist Conference (PVSC) (2015) 1–6, https://doi.org/10.1109/PVSC.2015.7355941.
[33] A.C. De Keizer, et al., PVSAT-2: Results of Field Test of the Satellite-Based PV System Perfomance Check, European Photovoltaic and Solar Energy Conference, 2006, pp. 2681–2685.
[34] Lorenz E., Betcke J., Drews A., Keizer A.C., Intelligent Performance Check of PV System Operation Based on Satellite Data (PVSAT-2), Final Technical Report 2007.
[35] n.d. Soda - Heliosat 2. http://www.soda-pro.com/help/helioclim/heliosat-2. (Accessed 6 May 2021).
[36] Rigollier C, Lefèvre M, Wald L. The method Heliosat-2 for deriving shortwave solar radiation from satellite images.
[37] GRASS GIS manual: r.sun n.d, https://grass.osgeo.org/grass76/manuals/r.sun.html. (Accessed 6 May 2021).
[38] Monedero J, García J, Dobon F, Yanes MA, Hernandez F. CALCULATION OF PV POTENTIAL MAPS IN THE CANARY ISLANDS.
[39] Linke turbidity factor - www.soda-pro.com n.d, http://www.soda-pro.com/gl/help/general-knowledge/linke-turbidity-factor (accessed June 26, 2021).
[40] Website Eulerhermes. https://www.eulerhermes.com/en_global/news-insights/economic-insights/Energy-prices-in-Europe-a-costly-winter-is-coming.html. (Accessed 26 December 2021).
[41] Wesite Xataka. https://www.xataka.com/energia/que-futuro-precio-luz-a-medio-plazo-tiene-mala-pinta-va-a-seguir-rompiendo-records-expertos. (Accessed 26 December 2021).
[42] Website Esios, Red Electrica de España. https://www.esios.ree.es/es/analisis/1739?vis=1&start_date=01-01-2021T00%3A00&end_date=31-12-2021T23%3A50&compare_start_date=01-12-2020T00%3A00&groupby=hour. (Accessed 28 December 2021).
[43] n.d. AEMET OpenData. https://opendata.aemet.es/centrodedescargas/inicio. (Accessed 8 May 2021).
[44] SIAR data n.d. https://eportal.mapa.gob.es//websiar/Inicio.aspx (accessed May 8, 2021).
[45] M. Luxan Garcia, A. Reymundo, Manual de diseño bioclimático para Canarias. http://mabican.itccanarias.org/pdf/ITC_MABICAN_Parte_II.pdf?b729e9f76aa4aa917dca63826637a37b=6a6ac55a52902c1bfc576d17c46425c3.